On the improvement of waves and storm surge hindcasts by downscaled atmospheric forcing: Application to historical storms

Émilie Bresson[1], Philippe Arbogast[1], Lotfi Aouf[2], Denis Paradis[2], Anna Kortcheva[3], Andrey Bogatchev[3], Vasko Galabov[3], Marieta Dimitrova[3], Guillaume Morvan[2], Patrick Ohl[2], Boryana Tsenova[3], and Florence Rabier[4]

[1]Centre National de Recherches Météorologiques - Groupe de Modélisation et d'Assimilation pour la Prévision, Toulouse, France
[2]Direction des Opérations pour la Prévision, Département Météorologie Marine et Océanographie, Météo-France, Toulouse, France
[3]National Institute of Meteorology and Hydrology, Sofia, Bulgaria
[4]European Centre for Medium-Range Weather Forecasts, Reading, United Kingdom

Correspondence to: Émilie Bresson (emilie.bresson@gmail.com)

Abstract. Winds, waves and storm surges can induce severe damages in coastal areas. To improve the preparedness to crisis due to such events a better knowledge of their statistical distribution is required. A better knowledge of past events is the first step to reach this purpose. This paper shows the use of atmospheric downscaling techniques in order to improve waves and storm surge hindcasts. Downscaling techniques are based on existing European Centre for Medium-Range Weather Forecasts reanalyses. The results show clearly that the 10 km-resolution wind forcing provided by the downscaled atmospheric model gives better waves and surges hindcast against using wind directly from the reanalysis. Furthermore, the analysis of the most extreme mid-latitude cyclones indicates that a 4-dimensional blending approach improves the whole process as it includes small scale processes in the initial conditions. Our approach has been successfully applied to ERA-20C (the twentieth century reanalysis).

1 Introduction

One of the most vulnerable areas affected by winter storms are coastal regions as their soils are often eroded and their population density is high (Barredo, 2007; Clarke and Rendell, 2009; Ferreira et al., 2009; Ciavola et al., 2011; André et al., 2013). Such storm events are frequently responsible for severe damages, huge economic losses and many casualties. Storm surges can reach 250 cm along the Atlantic coasts and 150 cm along the Western Black Sea coasts (Marcos et al., 2009; Ryabinin et al., 1996). Most winter storms that affect western Europe are associated with mid-latitude cyclones that originate in the Atlantic ocean (Klawa and Ulbrich, 2003; Della-Marta et al., 2009; Usbeck et al., 2010). The Bulgarian coasts are hit by cyclones whose origin lies in the Mediterranean (Bocheva et al., 2007). The cumulative effects of deep low pressures, dynamical action of winds and spring tides lead to a strong rise of sea level causing coastal flooding. For example, during the Xynthia storm which hit the western part of the French coast on February, 27^{th} 2010, this kind of combination occurred with a tide coefficient of 102, highest astronomical tide between 0.96 m and 1.15 m, and maximal recorded wind gusts of 160 km h^{-1} over coastal regions

and about 120 km h^{-1} over land (Rivière et al., 2012). Noteworthy storm surge reached more than 1.60 m at La Rochelle and Les Sables d'Olonne for this storm.

A better knowledge of the variability of these events is of primary interest to improve waves and storm surges warning systems. The trends in the frame of climate change are critical as well. Due to the lack of long-term wave records based on in-situ measurements and surge archives for the whole 20^{th} century, these wave and storm surge extreme events have to be reconstruct by hindcast using numerical models. A straightforward approach for hindcasting consists in using global atmospheric reanalyses as atmospheric forcing conditions of wave and storm surge numerical models (Reistad et al., 2011). A global atmospheric reanalysis is built using a data assimilation system and historical observations spanning an extended period. The Increasing Resilience through Earth Observation (IncREO) project offered the opportunity to test this approach for a limited number of wind storm cases studies. This project, funded by the Seventh Research Framework Programme (FP7) of the European Union, has brought together Earth observation data gathered through the European Union's programme Copernicus. This project makes those data available for emergency planning services and disaster management missions. One major component of the project consists in mapping of the coastal vulnerability using a series of past wave and surge extreme events.

In this study, we assess wave and storm surge hindcast for extreme events between 1924 and 2012. Thirty cases are selected to offer a large panel of extreme events with various affected areas (French Atlantic and Mediterranean coasts; Bulgarian Black Sea coasts), more or less extended impacted zones, different cyclone trajectories and amplitudes and varied highest astronomical tide (Tab. 1). The different European reanalyses (ERA), produced by European Centre for Medium-Range Weather Forecasts (ECWMF), have various period lenghts, model resolutions and assimilated datasets. ERA-20C, ERA-40 and ERA-Interim datasets are produced with a coupled climate system, including atmosphere, land surface and ocean (Tab. 2; Poli et al., 2013; Uppala et al., 2005; Dee et al., 2011). Although we can use the finer reanalysis as initial conditions for a given event, it turns out that mesoscale processes related to the formation of strong winds such as sting jets (Hewson and Neu, 2015) are absent even in ERA-Interim, the reanalysis with the highest resolution. As described in Reistad et al. (2011) and Li et al. (2016), a dynamical downscaling can be applied on these reanalyses using high resolution numerical model to better resolve the horizontal scales involved together in the mid-latitude cyclone development processes and interaction with fine resolution coastal topography. The purpose of this study is to present different downscaling approaches leading to better atmospheric forcings for wave and storm surge models and to assess the added value of those proposed approaches.

The paper is organized as follows. Section 2.1 describes the methodology and data used for the downscaling strategies; Section 2.2 presents wave and surge models configurations. Section 3 discusses the results: first examining the impact of the two downscaling techniques on a deep cyclone development; a second part is devoted to wave hindcasts evaluation; then storm surge model outputs skill is addressed; last part is dedicated to early 20^{th} century cases. Finally Section 4 summarizes the take-home messages.

2 Methodology

Mean sea level pressure and surface wind are needed as atmospheric forcing to forecast wave and storm surges. In the present study, these two variables are obtained through reanalyses built using a given data assimilation system constrained by past observations. A dynamical downscaling is applied on global atmospheric reanalyses since their resolution is too coarse to deliver accurate information for hindcast.

2.1 Dynamical downscaling of reanalyses

The general method of a dynamical downscaling uses a coarse resolution dataset, like global atmospheric reanalysis, as initial conditions for a numerical atmospheric model. Three ECMWF reanalyses are selected for this study: ERA-20C, ERA-40 and ERA-Interim (Tab. 2). They are all produced with a coupled climate system, incorporating atmosphere, land surface and ocean systems. ERA-40 includes conventional observations (e.g. surface stations, buoy, radiosondes), polar satellites and geostationary satellites. ERA-Interim datasets benefited of improvements in assimilation methods and large increase of available data. It turns out that observation quantity and quality increased with time. Therefore in order to mitigate the inhomogeneity of the 20^{th} century reanalysis, only observations of surface pressure and surface marine winds are assimilated in the ERA-20C dataset. To provide the best possible atmospheric conditions for wave and storm surge hindcast, the following ERA datasets are downscaled for each storm: ERA-20C for cases study before 1957, ERA-40 for 1957–1978 period, ERA-Interim for storms occurring in 1979 and after (Tab. 1).

Over both French and Bulgarian domains, numerical weather prediction (NWP) models need to assure high enough horizontal and time resolution especially for the storm surge model hindcast. For French events, the selected model, ARPEGE (Action de Recherche Petite Echelle Grande Echelle), is the operational global primitive-equation NWP system used at Météo-France and is based on the ARPEGE-IFS software developed in collaboration with ECMWF (Tab. 3; Courtier et al., 1991). A stretched grid allows a finer horizontal resolution over France (around 10 km) with a coarser one at the antipodes (60 km). The version used here has 70 hybrid vertical levels from 17 m to about 70 km. The Bulgarian events are hindcast thanks to ALADIN (Aire Limitée, Adaptation dynamique, Développement InterNational) for more consistency as the ARPEGE grid is too coarse over this region. ALADIN is a limited-area model based on the ARPEGE system (Radnóti et al., 1995). Its characteristics are the same as for ARPEGE.

Two dynamical downscaling methods (D1 and D2) are examined here. For D1, the necessary part from the global fields of ECMWF reanalysis are interpolated to the plane model domain both on horizontal and vertical for each NWP system (ARPEGE and ALADIN). The upper-air initialization step is using the spectral coefficients of ERA reanalyses. Then we apply the Schmidt transform which is well defined in spectral space to project the fields into the ARPEGE stretched grid. The land-surface initialization is not straightforward since many differences of land-surface parametrizations and physiographic databases between the two land-surface schemes can be found. For instance, the Tiled ECMWF Scheme for Surface Exchanges over Land (TESSEL) scheme of ERA uses four soil layers with fixed thicknesses, each layer having its own water content. The land-surface scheme of ARPEGE uses only two layers in our experiments, the top layer with a fixed size of 1 cm and

the second layer overlaps the first one and has a variable depth. For a given grid point soil types are very different in the two land-surface schemes. Therefore, using the raw land-surface datasets from ERA as initial conditions would be troublesome since the water saturation fraction depends on the soil type. Thus, we interpolate the surface fields so as to preserve as much as possible the surface heat and momentum fluxes (Boisserie et al., 2016). The procedure is based on the conservation of the Soil Wetness Index (a relevant indicator for soil water availability) during the interpolation process since soil water availability is supposed to regulate the partition of latent and heat fluxes, which, in turn, influence energy and water exchanges between the atmosphere and the land-surface. The resulting files are initial conditions for NWP forecasts and hourly forecasts are produced twice a day (at 00 UTC and 12 UTC), from H+06 to H+18. The first six hours are not taken into account to prevent model spin up, and after H+18, the next forecast time is considered. The D2 method helps to evaluate the importance of taking into account small wavelengths beyond the reanalysis truncation, not considered in D1. Furthermore, after a short period of time (3 hours), non-linearities trigger small scales which are consistent with the large scale. This small scale information provided by the 6-hour forecast is blended with the large scale given by the interpolated reanalysis (Fig. 1). This procedure was cycled 4 times. Therefore, the determination of one single initial condition uses 4 reanalyses and is then, in some sense, 4-dimensional. D2 technique is apply on 10 French events.

2.2 Description of wave and storm surge models

For more consistency, wave and storm surge models used here have similar general characteristics while being adapted to either French or Bulgarian coasts.

2.2.1 Wave models

The French coast extreme wave events are hindcast with the Meteo-France WAve Model (MFWAM), a third-generation model of the operational wave forecasting system of Météo-France (Tab. 3). This model is based on the IFS-CY36R4 of the European wave model (ECWAM) with modified source terms for the dissipation by wave breaking and the air friction dedicated to swell damping as described in Ardhuin et al. (2010). The MFWAM model uses the wind input term developed as defined in Bidlot et al. (2005). The dissipation by wave breaking is directly related to the wave spectrum with a saturation rate of dissipation. The source term is a combination of an isotropic part and a direction-dependent part that controls the directional spread of the resulting wave spectra. It includes a cumulative effect describing the smoothing of big breakers on small breakers. The term also uses a wave turbulence interaction part, which is weak as indicated in Ardhuin et al. (2010). The MFWAM model uses a quadruplet non linear interaction term based on the discrete interactions approximation as indicated in the ECWAM model. In this study, a nested MFWAM model is implemented with a grid size of 0.1° for western European seas including the Mediterranean Sea. The domain boundaries are 20° N-72° N, 32° W-42° E for latitude and longitude, respectively (EURAT01 domain in Fig 2). The wave spectrum is discretized in 24 directions and 30 frequencies starting from 0.035 to 0.58 Hz. This regional model is forced by boundary conditions provided by the global MFWAM model with a grid size of 0.5°. The global MFWAM model is driven by 6-hourly ERA winds reanalyses.

The SWAN (Simulating Waves Nearshore) model is used for the Bulgarian cases (Tab. 3). It is a third-generation wave model that is especially designed to simulate waves in near shore waters and is very often applied to enclosed and semi-enclosed seas, estuaries and lakes (Booij et al., 1999). The model computes random, short-crested wind-generated waves in coastal regions and inland waters. SWAN accounts for wave propagation and transitions from deep to shallow water at finite depths by solving the spectral wave action balance equation, which includes source terms for the wind input, non-linear interactions, white-capping, bottom friction and depth-induced breaking. The model performance, the parameterizations of the wave generation and dissipation processes and other aspects of SWAN applied to the Black Sea have been studied by Akpinar et al. (2012); Arkhipkin et al. (2014); Rusu et al. (2014). The model domain that is used for the simulations of historical Black Sea storms is based on a numerical grid covering the entire Black Sea area (40° N-47° N and 27° E-42° E; hereafter named BUL; Fig. 2) with a mesh size of 0.0333° in latitude and longitude. The spectral discretization is based on 36 directions and 30 frequencies logarithmically spaced from 0.05 Hz to 1.00 Hz. The wind input parameterization follows Komen et al. (1984) and white-capping is based on Hasselmann (1974) with the δ coefficient (which determines the dependency of white-capping on wave number) set to 1 (according to the study by Rogers et al., 2003). This specific set of parameterizations is chosen to have the lowest bias, root mean square error (RMSE) and scatter index when comparing results from the model and the along-track satellite altimetry data.

2.2.2 Storm surge models

The operational surge model of Météo-France (Daniel et al., 2001) is a barotropic 2-dimensional version of the HYCOM model (HYbrid Coordinate Ocean Model) implemented by SHOM (Service Hydrographique et Océanographique de la Marine) from the 3-dimensional version (Tab. 3; Bleck, 2002; Baraille and Filatoff, 1995). The HYCOM code is managed by an international consortium: COAPS (Center for Ocean-Atmospheric Prediction Studies; USA), NRL (Naval Research Laboratory; USA), SHOM (France), DMI (Danish Meteorological Institute; Denmark) and NERSC (Nansen Environmental and Remote Sensing Center; Norway). The model is run on two domains (Fig. 2): ATL corresponds to the North-East Atlantic area (Bay of Biscay, English Channel and North Sea), from 9° W to 10° E and from 43° N to 62° N; MED defines the Mediterranean Sea domain, from 9° W to 37° E and from 30° N to 46° N; with a grid size of around 1 km on the French coast (curvilinear grid). The tides imposed at the marine boundaries are computed thanks to 17 harmonic components from the COMAPI (COastal Modelling for Altimetry Product Improvement project) regional atlas implemented in the North East Atlantic Ocean area (Cancet et al., 2010); the bottom friction coefficient is spatially variable and has been optimized to properly reproduce the propagation of tides. Tides are discarded in the storm surge computation, and another computation of the tides, based in harmonic components obtained from measurements by SHOM, is added to the storm surge in order to know the sea level with more accuracy, at specific locations. The bottom friction coefficient is constant and taken equal to 0.002. For both HYCOM configurations (ATL and MED), the drag coefficient used to compute the wind stress, follows the Charnock (1955) scheme with a constant Charnock parameter of 0.025.

The simulations of storm surges for Black Sea cases are based on the storm surge model of Météo-France (Daniel et al., 2001) adapted to the Black Sea by Mungov and Daniel (2000) (Tab. 3). The model is depth-integrated, and tides are not taken

into account as their amplitude is less than 9 cm in the Black Sea. The model grid for the Black Sea is a regular spherical grid with a spatial resolution of 0.0333°. The model domain covers the entire Black Sea. The bottom friction coefficient is 1.5 10^{-3} over the shelf and 1.5 10^{-5} over the liquid bottom. The depth of the Black Sea mixed layer is considered as a liquid bottom (given the very stable stratification of the Black Sea waters and the shallowness of the mixed layer depth). Data about the seasonal variations of the Black Sea mixed layer depth are taken from the study by Kara et al. (2009). Without this specific set-up of a liquid bottom, the depth integrated models for the Black Sea would fail to simulate any surge even if very strong, constant winds were used as an input. The bathymetry data for the storm surge model (and the wave model) are obtained by digitalization of proprietary maps provided by the Bulgarian military hydrographic service.

3 Results

3.1 Impact of the two downscaling techniques on a deep cyclone development

The effects of two downscaling techniques on the reconstruction of intense storms are presented with an example of a deep cyclone development. The Lothar storm was an extreme cyclogenesis event occurring a few hours before the Martin storm in December 1999. It is the most extreme storm in terms of pressure gradient, surface wind and displacement velocity to hit France to this day (Wernli et al., 2002; Rivière et al., 2010). This storm did not produce extreme wave and storm surge, thus it was not selected for hindcasts. Nevertheless it is interesting to look at the behaviour oh both downscaling strategies for this case where the horizontal pressure gradient are so strong. Fig. 3 shows the comparison of the downscaling strategies applied to this storm. D1 improves the ERA-Interim reanalysis fields but D2 better reproduces the cyclone structure over Northern France than D1 and the ERA reanalysis. Statistics are performed with the 12 meteorological stations available on an area encompassing the low (48° N-50° N; 2° E-4° E). Table 4 confirms that downscaling is noticeably better than using an ERA-Interim reanalysis in regard to surface observations. Table 4 also highlights the slight improvement of results by the use of D2.

The purpose of the paper is to measure to what extent the mesoscale features built by the downscaling techniques beyond the reanalysis truncation have an impact in terms of surge and wave reconstruction.

3.2 Wave hindcasts

Significant wave heights (SWH) hindcasts can be evaluated by using, for example, in-situ observations and satellite altimeter data. Several satellites operated while some selected storms occurred: TOPEX-Poseidon (1992–2005), ENVISAT (2002–2012), Jason-1 (2002–2013) and Jason-2 (2008–). Buoys and Acoustic Doppler Current Profiler (ACDP) provide SWH information as well. Caveats remaining in each of these observations datasets together with the coarse resolution of altimeter measurements do not enable a comprehensive verification for all the selected cases. The simulated wave heights are collocated with the altimeter tracks with a time window of 3 hours. For the 2004, 2007, 2008 and 2010 storms, data are collected from three altimeters: Jason-1, Envisat and Jason-2. Fig. 4 shows the scatter plots between model and altimeter wave heights. This clearly indicates that the use of D1 winds induces a better fit with a strong reduction of normalized root mean square error (NRMSE) from 17.1

to 13.1 %. The bias is also significantly reduced from -35 to -4 cm. The best performance of the MFWAM model with D1 winds is obtained for the 2008 storm, where the NRMSE of SWH is significantly reduced from 15.9 to 11.8 % with D1, as illustrated in Fig. 5. The statistical analysis reveals that the use of D2 winds leads to better results than the use of interpolated ERA winds. Biases of SWH are slightly improved using D2 winds rather than when using D1 winds. However, D2 winds slightly increases the NRMSE of SWH for the 2004, 2007 and 2008 storms. Only for the storm Xynthia (February 2010), the D2 winds improve slightly the NRMSE of significant wave height. The evaluation with altimeters does not show clearly a gain from using the advanced D2 technique against D1. It seems that D2 shows better skills for higher wind speeds such as the ones observed during the Lothar storm. For the 1998, 1999 and 2000 storms, altimeters wave heights from TOPEX and ERS2 are used for the evaluation of the modelled wave heights. The same tendency is found with a strong decrease of NRMSE of SWH from 16.2 to 14.1 %, and the bias is well reduced from -32 to 10 cm (not shown). The SWH hindcast and measured by the buoys are also compared for the most recent storms. Fig. 6 shows time series of SWH from model and buoys at the peak of the storm on February 2010 at Nice (43.4° N and 7.8° E) on the Mediterranean coast. This indicates a good fit on SWH induced by using D1 winds comparing to interpolated ERA winds. The February 2012 storm is presented as an example of evaluation. The wave model outputs are evaluated by comparing the simulated SWH with along-track data measured by the Jason-1 and ENVISAT satellite altimeters on 7 and 8 February 2012. The SWAN model output is compared to the satellite altimeter data from the Jason-1 and ENVISAT satellites. Four satellite tracks crossed the area with high waves in the western Black Sea (the total number of data points along the tracks was 214). Although this small number of data points, this event is the only opportunity to evaluate the SWAN model outputs. For the Black Sea, the occurrence of a storm seldom happens when more than one satellite track crosses the area with the highest waves. The results of the comparison of the modelled SWH simulations with the ENVISAT satellite altimetry along-track data are presented in Table 5 and Fig. 7. Statistics have shown that the use of D1 forcing improves the wave hindcast (Table 5). The highest waves, obtained with D1 forcing, reached about 7 m south of Ahtopol, where unfortunately the storm destroyed the tide gauge and the measurements were therefore lost. As a consequence, the SWAN model output, in terms of significant wave height, is compared with in-situ wave measurements by ADCP located at Pasha Dere beach at 20 m depth. The data was provided by the Bulgarian Institute of Oceanology (Valchev et al., 2014). Fig. 8 presents a comparison of the wave measurements with the SWAN model outputs, obtained using the two wind inputs as an atmospheric forcing. Clearly the use of D1 slightly overestimates the measured wave heights. The use of ERA-Interim underestimates drastically the modelled values of significant wave height, while the use of D1 winds leads to better matching of the simulated and measured wave heights. To conclude, the use of D1 winds considerably improved the bias, the root mean square error and the scatter index of significant wave height for this severe storm.

3.3 Storm surge hindcasts

Storm surge hindcasts can be evaluated by tide gauges measurements. A network of 25 tide gauges around the French coasts is maintained to validate surge model implemented at Météo-France; 12 hydro-meteorological stations are located along the Bulgarian coasts. Depending of the storm spread and instrument condition, the number of available data is different for each storm. For a global evaluation of hindcast regarding tide gauges, all the available measurements with a peak in storm surge

are selected. A Weighted Normalized Observation Error ($WNOE$) is calculated to highlight over and underestimation of simulated maximum storm surges regarding measurements. It is defined by:

$$WNOE = 100.\alpha(t).\left(\frac{X_{sim} - X_{mea}}{X_{mea}}\right) \quad (1)$$

with $\alpha(t) = 1.1$ if $t_{mea} - 3 < t_{sim} < t_{mea} + 3$ and $\alpha(t) = 0.9$ otherwise.

$X_{sim(mea)}$ is the simulated (measured) value of maximum storm surge (in cm); $t_{sim(mea)}$ is the corresponding time (in hours); α is the weighting coefficient. α is equal to 0.9 if the simulated maximum of storm surge is in a window of +/- 3 h regarding observed peak time; if it is sooner or later, the bias is multiplied by 1.1. For some cases, when no time information is available, no weighting is applied, thus α = 1. Fig. 9 presents the percentage of events regarding their WNOE value. A tendency of underestimation by using ERA forcing is highlighted in comparison of forcing models with D1 or D2 atmospheric outputs. When considering extreme cases only, those with low or moderate errors (say $\|WNOE\| < 20\%$) represent respectively 18%, 63% and 69% for ERA, D1 and D2. Dispersion of D2 results is larger then for D1. Table 6 presents the portion of cases in the satisfactory range ($\|WNOE\| < 20\%$) for each coastline and for cases studied with the three different forcing. Values have to be evaluated regarding the number of samples presented in Tab. 7. For each coastline, D1 and D2 lead to better result than with ERA. Atlantic cases are better performed with D2. The ability of D2 to simulate very deep cyclones could explained this point.

A special focus is now made on the storm occurring on December 2004 which mostly affects the British Channel and the North Sea. Following a deep low of 980 hPa which crossed from West to East the North French coasts, the wind increased veering north-westerly on nearby seas, generating high waves and surge along the coast. The maximum surge exceeds 1 m at St Malo and Dunkirk, and fortunately under average tide, as illustrated in Fig. 10. During this event, it is clearly shown that the use of D1 forcing captures the peak of the surge in St Malo and Dunkirk (Fig. 10) whereas ERA winds induces an underestimation of the surge by roughly 60 cm and 20 cm at St Malo and Dunkirk, respectively. The use of D2 winds induces an overestimation of the surge of 20 cm at St Malo. At Dunkirk, the storm surge from D1 and D2 gives almost the same surge. Another example of storm surge hindcast is the November 2007 storm. It affected the whole domain of North Sea (Dunkirk and Calais on the French coast), and slightly the East British channel. It is associated to a strong north-westerly flux on the North Sea and lasted nearly 24 hours. At the peak of the storm event, a surge of 2.30 m is recorded at Dunkirk, as illustrated in Fig. 11. This also shows the good fit obtained by the model with the two wind forcing D1 and D2. However the ERA forcing was significantly underestimating the surge by 80 cm (Fig. 11). One can see for this storm that D2 winds give slightly better surge results on 11 November 2007 at 00 UTC. These two storms are an example of the various response of the storm surge hindcast with both types of downscaling: no significant trend could be highlighted.

3.4 Evaluation of early 20^{th} century cases hindcast using ERA-20C

Twentieth century extreme events which occurred before 1957 can be hindcast by using ERA-20C, the 20^{th} century reanalysis ECMWF project (Poli et al., 2013). For these cases, even if there were no available wave observations , a storm surge evaluation is possible thanks to reliable sea level observations.

To validate the concept of downscaling using ERA20C analyses, a focus is made on the major storm which occurred in the North Sea in February 1953 (Fig. 12), which caused severe damages to the Dutch, Belgian and English coasts. Wind intensity around force 10 on the Beaufort scale (around 50 kt) were measured in Scotland and Northern England. The winds and the low pressures combined with exceptional spring tides and the funnel shape and shallowness of the North Sea were responsible for the surge. The Netherlands were the worst affected, recording 1,836 deaths and widespread property damage (Gerritsen, 2005). Most of the casualties occurred in the southern province of Zeeland. Three hundred and seven people were killed in England, 19 in Scotland and 28 in Belgium. The MFWAM results using the D1 winds indicate SWH exceeding 16 m in the western part of the North Sea at 00 UTC on 1 February 1953 (Fig. 13). The most striking fact is the long strong swell with a peak period of 20 s, which hit the Dutch coasts inducing wave flooding. The storm surge simulation shows a very high surge which is very unusual for this area: along the Dutch and Belgian coastlines storm surges exceeded 3 m (Fig. 14). Fig. 15 shows the comparison of the storm surges obtained with ERA-20C and D1 forcing with observations recorded at four locations. The improvement induces by D1 forcing particularly marked at Ijmuiden, Ostend, Brouwershavn and Dieppe where recorded peaks of storm surge are well caught when compared to ERA-20C.

4 Conclusions

ECMWF reanalyses are widely used for many climatological studies. However, their coarse spatial resolution and the limited access in term of time frequency of model output generate strong uncertainties for high wind speed associated with extreme mid-latitude cyclones. To overcome this problem, dynamical downscaling techniques are implemented and applied to reproduce high resolution historical atmospheric fields. ERA-20C, ERA-40 and ERA-Interim are used to encompass the 1924 – 2012 studied period. Very short range forecasts using 10 km resolution and hydrostatic models initialized with ERA analyses provide downscaled MSLP and 10 m wind fields which are used in turn to force wave and storm surge numerical models. This approach was already experimented for the North Sea coast for a long period using only ERA-40.

To evaluate such a technique on different initial conditions, thirty cases are selected over French and Bulgarian coastlines to offer a large panel of characteristics: location, intensity, highest astronomic tide, meteorological context. Some early 20^{th} century cases generating extreme storm surge and waves are part of this selection thanks to ERA-20C recent availability. This study shows a significant and quasi-systematic improvement of wave and storm surge hindcast when using downscaled winds. The evaluation with independent wave observations such as wave heights from altimeters shows the strong reduction of bias and improved RMSE of significant wave height for extreme waves events. The downscaling techniques are also well suited to storm surge extreme events, such as the 1953 storm since the storm surge reconstruction using the present approach fits with the recorded data at the Belgian and Dutch coasts. The D2 method, generally leads to an improvement in comparison with D1, especially for cases with small-scale, intense, mid-latitude cyclones.

Downscaling is a very promising technique to provide an accurate reconstruction of waves and storm surges for the whole 20^{th} century. After evaluation and calibration with observations, these model outputs can be very useful to analyse the inter-annual variability of the coastal consequences of wind-storms and to improve the thresholds used in the wave submersion

warning system. Further, regional climate modelling is expected to address the response of wave and surge extreme variability to storm-track modifications due to global change. A further step towards this objective would be to use interactive model of wave and storm surge to enhance hindcast. Consequently, all these points will open applications for coastal protection and risk management.

Acknowledgements. The research was carried out as part of the IncREO (Increasing Resilience through Earth Observation) project with funding from the European Union Seventh Framework Programme under the grant agreement n°312461. The authors would like to thank the European Commission for its financial support through the 7th framework programme project. We are also most grateful to Françoise Taillefer for her unconditional technical support and François Bouyssel for his constructive and valuable advice about the second downscaling method. Special thanks go to Philippe Dandin for his involvement in setting up this project. We also thank SHOM for providing the French storm surge measurements. Jean Maziejewski are warmly thanked for helping to improve the manuscript

References

Akpinar, A., van Vledder, G. P., Kömürcü, M. I., and Özger, M.: Evaluation of the numerical wave model (SWAN) for wave simulation in the Black Sea, Cont. Shelf Res., 50, 80–99, https://doi.org/10.1016/j.csr.2012.09.012, 2012.

André, C., Monfort, D., Bouzit, M., and Vinchon, C.: Contribution of insurance data to cost assessment of coastal flood damage to residential buildings: insights gained from Johanna (2008) and Xynthia (2010) storm events, Nat. Hazards Earth Syst. Sci., 13, 2003–2012, 2013.

Ardhuin, F., Rogers, E., Babanin, A., Filipot, J.-F., Magne, R., Roland, A., Westhuysen, A. V. D., Queffeulou, P., Lefevre, J.-M., Aouf, L., and Collard, L.: Semi-empirical dissipation source functions for ocean waves : Part 1, definition, calibration and validation, J. Phys. Oceanogr., 40, 1917–1941, 2010.

Arkhipkin, V. S., Gippius, F. N., Koltermann, K. P., and Surkova, G. V.: Wind waves in the Black Sea: results of a hindcast study, Nat. Hazards Earth Syst. Sci., 14, 2883–2897, https://doi.org/10.5194/nhess-14-2883-2014, 2014.

Baraille, R. and Filatoff, N.: Modèle shallow-water multicouches isopycnal de Miami, Tech. Rep. 003/95, SHOM/CMO, 1995.

Barredo, J. I.: Major flood disasters in Europe: 1950–2005, Natural Hazards, 42, 125–148, 2007.

Bidlot, J., Janssen, P., and Abdalla, S.: On the importance of spectral wave observations in the continued development of global wave models, in: Proc. 5th. Int. Symposium on Ocean Wave Measurements and Analysis (WAVES 2005), 2005.

Bleck, R.: An oceanic general circulation model framed in hybrid isopycnic - Cartesian coordinates, Ocean modelling, 4, 55–88, https://doi.org/10.1016/S1463-5003(01)00012-9, 2002.

Bocheva, L., Georgiev, C. G., and Simeonov, P.: A climatic study of severe storms over Bulgaria produced by Mediterranean cyclones in 1990- 2001 period, Atmos. Res., 83, 284–293, 2007.

Boisserie, M., Decharme, B., Descamps, L., and Arbogast, P.: Land surface initialization strategy for a global reforecast dataset, Quart. J. Roy. Meteor. Soc., 142, 880–888, https://doi.org/10.1002/qj.2688, http://dx.doi.org/10.1002/qj.2688, 2016.

Booij, N., Ris, R. C., and Holthuijsen, L. H.: A third-generation wave model for coastal regions: 1. Model description and validation, Journal of geophysical research: Oceans, 104(C4), 7649–7666, 1999.

Cancet, M., Lux, M., Pénard, C., Lyard, F., Birol, F., Lemouroux, J., Bourgogne, S., and Bronner, E.: COMAPI: New regional tide atlases and high frequency dynamical atmospheric correction, in: Ocean Surface Topography Science Team meeting, 2010.

Charnock, H.: Wind Stress on a Water Surface, Quart. J. Roy. Meteor. Soc., 81, 639–640, 1955.

Ciavola, P., Ferreira, O., Haerens, P., Van Koningsveld, M., Armaroli, C., and Lequeux, Q.: Storm impacts along European coastlines. Part 1: The joint effort of the MICORE and ConHaz Projects, Environmental Science & Policy, 14, 912–923, 2011.

Clarke, M. L. and Rendell, H. M.: The impact of North Atlantic storminess on western European coasts: a review, Quaternary International, 195, 31–41, 2009.

Courtier, P., Freydier, C., Geleyn, J.-F., Rabier, F., and Rochas, M.: The ARPEGE project at Météo-France, ECMWF Annual Seminar, Eur. Cent. for Medium-Range Weather Forecasts, Reading, U. K, 1991.

Daniel, P., Josse, P., and Ulvoas, V.: Atmospheric forcing impact study in Meteo-France storm surge model. In: Coastal engineering V, computer modeling of seas and coastal regions, Wessex, UK: WIT Press., 2001.

Dee, D. P., Uppala, S. M., Simmons, A. J., Berrisford, P., Poli, P., Kobayashi, S., Andrae, U., Balmaseda, M. A., Balsamo, G., Bauer, P., Bechtold, P., Beljaars, A. C. M., van de Berg, L., Bidlot, J., Bormann, N., Delsol, C., Dragani, R., Fuentes, M., Geer, A. J., Haimberger, L., Healy, S. B., Hersbach, H., Hólm, E. V., Isaksen, L., Kållberg, P., Köhler, M., Matricardi, M., McNally, A. P., Monge-Sanz, B. M., Mor-

crette, J.-J., Park, B.-K., Peubey, C., de Rosnay, P., Tavolato, C., Thépaut, J.-N., and Vitart, F.: The ERA-Interim reanalysis: configuration and performance of the data assimilation system, Quart. J. Roy. Meteor. Soc., 137, 553–597, https://doi.org/10.1002/qj.828, 2011.

Della-Marta, P. M., Mathis, H., Frei, C., Liniger, M. A., Kleinn, J., and Appenzeller, C.: The return period of wind storms over Europe, International Journal of Climatology, 29, 437–459, 2009.

Ferreira, Ó., Ciavola, P., Armaroli, C., Balouin, Y., Benavente, J., Río, L. D., Deserti, M., Esteves, L., Furmanczyk, K., Haerens, P., et al.: Coastal storm risk assessment in Europe: examples from 9 study sites, J. Coastal Res., pp. 1632–1636, 2009.

Gerritsen, H.: What happened in 1953? The Big Flood in the Netherlands in retrospect, Philosophical Transactions of the Royal Society of London A: Mathematical, Physical and Engineering Sciences, 363, 1271–1291, https://doi.org/10.1098/rsta.2005.1568, http://rsta.royalsocietypublishing.org/content/363/1831/1271, 2005.

Hasselmann, K.: On the spectral dissipation of ocean waves due to white-cap, Boundary-Layer Meteorology, 6 (1-2), 107–127, 1974.

Hewson, T. D. and Neu, U.: Cyclones, windstorms and the IMILAST project, Tellus A: Dynamic Meteorology and Oceanography, 67, 27 128, 2015.

Kara, A. B., Helber, R. W., Boyer, T. P., and Elsner, J. B.: Mixed layer depth in the Aegean, Marmara, Black and Azov Seas: Part I: General features, J. Marine Syst., 78, 169–180, https://doi.org/10.1016/j.jmarsys.2009.01.022, 2009.

Klawa, M. and Ulbrich, U.: A model for the estimation of storm losses and the identification of severe winter storms in Germany, Nat. Hazards Earth Syst. Sci., 3, 725–732, 2003.

Komen, G. J., Hasselmann, S., and Hasselmann, K.: On the existence of a fully developed wind sea spectrum, J. Phys. Oceanogr., 14, 1271—-1285, 1984.

Li, N., Cheung, K. F., Stopa, J. E., Hsiao, F., Chen, Y.-L., Vega, L., and Cross, P.: Thirty-four years of Hawaii wave hindcast from downscaling of climate forecast system reanalysis, Ocean Model., 100, 78–95, 2016.

Marcos, M., Tsimplis, M. N., and Shaw, A. G.: Sea level extremes in southern Europe, Journal of Geophysical Research: Oceans, 114, 2009.

Mungov, G. and Daniel, P.: Storm-surges in the Western Black Sea. Operational forecasting, J. Mediterranean Marine Science, 1 (1), 45–51, 2000.

Poli, P., Hersbach, H., Tan, D., Dee, D., Thépaut, J.-N., Simmons, A., Peubey, C., Laloyaux, P., Komori, T., Berrisford, P., Dragani, R., Trémolet, Y., Holm, E., Bonavita, M., Isaksen, L., and Fisher, M.: The data assimilation system and initial performance evaluation of the ECMWF pilot reanalysis of the 20th-century assimilating surface observations only (ERA-20C), Tech. rep., ECMWF, 2013.

Radnóti, G., Ajjaji, R., Bubnová, R., Caian, M., Cordoneanu, E., Von Der Emde, K., Gril, J., Hoffman, J., Horányi, A., Issara, S., et al.: The spectral limited area model ARPEGE-ALADIN, PWPR report series, pp. 111–117, 1995.

Reistad, M., Breivik, Ø., Haakenstad, H., Aarnes, O. J., Furevik, B. R., and Bidlot, J.-R.: A high-resolution hindcast of wind and waves for the North Sea, the Norwegian Sea, and the Barents Sea, Journal of Geophysical Research: Oceans, 116, 2011.

Rivière, G., Arbogast, P., Maynard, K., and Joly, A.: The essential ingredients leading to the explosive growth stage of the European wind storm Lothar of Christmas 1999, Quart. J. Roy. Meteor. Soc., 136, 638–652, 2010.

Rivière, G., Arbogast, P., Lapeyre, G., and Maynard, K.: A potential vorticity perspective on the motion of a mid-latitude winter storm, Geophys. Res. Lett., 39, https://doi.org/10.1029/2012GL052440, 2012.

Rogers, W. E., Hwang, P. A., and Wang, D. W.: Investigation of wave growth and decay in the SWAN model: three regional-scale applications, J. Phys. Oceanogr., 33, 366–389, 2003.

Rusu, L., Butunoiu, D., and Rusu, E.: Analysis of the extreme storm events in the Black Sea considering the results of a ten-year wave hindcast, J. environ. prot. ecol., 15, 445–454, 2014.

Ryabinin, V. E., Zilberstein, O. I., and Seifert, W.: Storm surges, World Meteorological Organization, 1996.

Uppala, S. M., KÅllberg, P. W., Simmons, A. J., Andrae, U., Bechtold, V. D. C., Fiorino, M., Gibson, J. K., Haseler, J., Hernandez, A., Kelly, G. A., Li, X., Onogi, K., Saarinen, S., Sokka, N., Allan, R. P., Andersson, E., Arpe, K., Balmaseda, M. A., Beljaars, A. C. M., Berg, L. V. D., Bidlot, J., Bormann, N., Caires, S., Chevallier, F., Dethof, A., Dragosavac, M., Fisher, M., Fuentes, M., Hagemann, S., Hólm, E., Hoskins, B. J., Isaksen, L., Janssen, P. A. E. M., Jenne, R., Mcnally, A. P., Mahfouf, J.-F., Morcrette, J.-J., Rayner, N. A., Saunders, R. W., Simon, P., Sterl, A., Trenberth, K. E., Untch, A., Vasiljevic, D., Viterbo, P., and Woollen, J.: The ERA-40 re-analysis, Quart. J. Roy. Meteor. Soc., 131, 2961–3012, https://doi.org/10.1256/qj.04.176, 2005.

Usbeck, T., Wohlgemuth, T., Pfister, C., Volz, R., Beniston, M., and Dobbertin, M.: Wind speed measurements and forest damage in Canton Zurich (Central Europe) from 1891 to winter 2007, Int. J. Climatol., 30, 347–358, 2010.

Valchev, N., Andreeva, N., Eftimova, P., and Trifonova, E.: Prototype of Early Warning System for coastal storm hazard (Bulgarian Black Sea Coast), CR Acad Bulg Sci, 67, 977, 2014.

Wernli, H., Dirren, S., Liniger, M. A., and Zillig, M.: Dynamical aspects of the life cycle of the winter storm 'Lothar'(24–26 December 1999), Quart. J. Roy. Meteor. Soc., 128, 405–429, 2002.

Table 1. List of the 30 cases selected for this study. Coast: Atl. - Med. for Atlantic and Mediterranean. Tide gauges: number of available and useful tide gauges. Storm surge (m): maximum storm surge recorded. Star is for unknown information.

Coast	Date	Tide gauges	Storm surge	Downscaling	ERA reanalyses
Atlantic	8 Oct. 1924	*	*	D1	ERA-20C
	14 Mar. 1937	*	*	D1	ERA-20C
	31 Jan - 1 Feb. 1953	*	> 3	D1	ERA-20C
	13 Feb. 1972	10	1.83	D1	ERA-40
	30 Nov. - 2 Dec. 1976	12	1.36	D1	ERA-40
	11 - 13 Jan. 1978	7	1.65	D1	ERA-40
	15 - 16 Oct. 1987	12	1.72	D1	ERA-Interim
	26 Feb. - 1 Mar. 1990	6	1.67	D1	ERA-Interim
	2 - 4 Jan. 1998	5	1.60	D1 / D2	ERA-Interim
	6 Nov. 2000	8	1.00	D1 / D2	ERA-Interim
	17 Dec. 2004	7	1.30	D1 / D2	ERA-Interim
	9 Nov. 2007	2	2.20	D1 / D2	ERA-Interim
	10 Mar. 2008 (Johanna)	7	1.30	D1 / D2	ERA-Interim
	23 - 24 Jan. 2009 (Klaus)	10	1.29	D1	ERA-Interim
	28 Feb. 2010 (Xynthia)	8	> 1.60	D1 / D2	ERA-Interim
Mediterranean	6 Nov. 1982	*	*	D1	ERA-Interim
	6 - 7 Feb. 2009	7	0.60	D1 / D2	ERA-Interim
	24 - 25 Dec. 2009	6	0.50	D1 / D2	ERA-Interim
	19 Feb. 2010	6	0.50	D1 / D2	ERA-Interim
Atl. - Med.	27 Dec. 1999 (Martin)	4	1.60	D1 / D2	ERA-Interim
Bulgarian	5 - 21 Oct 1976	2	1.00	D1	ERA-40
	16 - 21 Jan. 1977	1	0.60	D1	ERA-40
	13 - 23 Feb. 1979	3	1.43	D1	ERA-Interim
	7 - 10 Jan. 1981	0	*	D1	ERA-Interim
	24 - 31 Dec. 1996	2	1.00	D1	ERA-Interim
	15 - 19 Dec. 1997	1	1.30	D1	ERA-Interim
	20 - 27 Jan. 1998	2	0.90	D1	ERA-Interim
	1 - 3 Jul. 2006	2	0.60	D1	ERA-Interim
	8 - 11 Mar. 2010	2	0.90 - 1.00	D1	ERA-Interim
	7 - 9 Feb. 2012	2	*	D1	ERA-Interim

Table 2. Characteristics of ERA-20C, ERA-40 and ERA-Interim reanalyses. 4(3)D-Var: 4(3)-dimensional variational analysis; VarBC: Variational Bias Correction of surface pressure observations.

	ERA-20C	ERA-40	ERA-Interim
Time period	1900 – 2010	1957 – 2002	1979 – present
IFS version	Cy38r1	Cy23r4	Cy31r2
Data assimilation system	24-hour 4D-Var; VarBC	6-hour 3D-Var	12-hour 4D-Var; VarBC
Spectral resolution	T159 ($\sim$ 125 km)	T159 ($\sim$ 125 km)	T255 ($\sim$ 80 km)
Number of vertical levels	91	60	60
Vertical scale (from the surface up to)	0.01 hPa ($\sim$ 80 km)	0.1 hPa ($\sim$ 64 km)	0.1 hPa ($\sim$ 64 km)
Pressure levels	37	23	37
Reference	Poli et al. (2013)	Uppala et al. (2005)	Dee et al. (2011)

Table 3. Outline of the numerical models required for wave and storm surge hindcasts.

Purpose	Model	Resolution	Coupling - Initial conditions data	Domain
Atmosphere	ARPEGE D1	T798 ($\sim$ 10 km)	ERA	global
	ARPEGE D2	T798 ($\sim$ 10 km)	ERA + ARPEGE	global
	ALADIN	10km	ARPEGE D1	Bulgaria
Wave	MFWAM	0.1°	ARPEGE D1/D2	Western Europe
	SWAN	0.1°	ALADIN	Bulgaria
Surge	HYCOM	1 km	ARPEGE D1/D2 + bathymetry	ATL
	HYCOM	1 km	ARPEGE D1/D2 + bathymetry	MED
	MF model	0.0333°	ALADIN + bathymetry	Black Sea

Table 4. Statics for MSLP from ERA reanalysis at 06 UTC 26 December 1999, 12-h forecast using the D1 and D2 at 18 UTC 25 December 1999, versus observations at 06 UTC 26 December 1999. Mean (hPa), standard deviation error (STD; hPa), bias (hPa), Root Mean Square Error (RMSE; hPa). Calculations are done for the nearest point. Small domain corresponds to 48° N-50° N; 2° E-4° E and includes 12 pairs of data and model values.

	Mean	STD	Bias	RMSE
Obs	973	2	–	–
ERA	993	10	12	18
D1	980	1	6	6
D2	977	1	5	5

Table 5. Comparison of SWAN wave model SWH (m) and altimeter data from ENVISAT and JASON1 satellites for the 2012 case over Bulgarian coast.

Time of satellite track		Pairs	Mean			Biais		RMSE		Scatter Index	
			Obs	ERA	D1	ERA	D1	ERA	D1	ERA	D1
7 Feb. 2012	08 UTC	44	3.9	3.5	4.1	-0.43	0.21	0.60	0.37	0.15	0.10
	14 UTC	76	3.6	3.2	3.8	-0.41	0.15	0.66	0.57	0.18	0.16
	20 UTC	51	6.4	5.3	6.3	-1.08	-0.09	1.14	0.37	0.18	0.06
8 Feb. 2012	14 UTC	43	5.6	4.4	4.7	-1.22	-0.94	1.37	1.16	0.24	0.21

Table 6. Portion of cases (%) with $\|WNOE\| < 20\%$ for each coast (ATL: Atlantic; MED: Mediterranean Sea; BUL: Bulgarian; common cases: cases using D1 and D2 forcing).

	ERA	D1	D2
ATL	21	63	80
MED	0	54	38
BUL	33	100	–
Common cases	18	64	61

Table 7. Number of observations used for calculations of $WNOE$ for each region and each forcing.

	ERA	D1	D2
ATL	34	34	15
MED	13	13	13
BUL	9	9	0

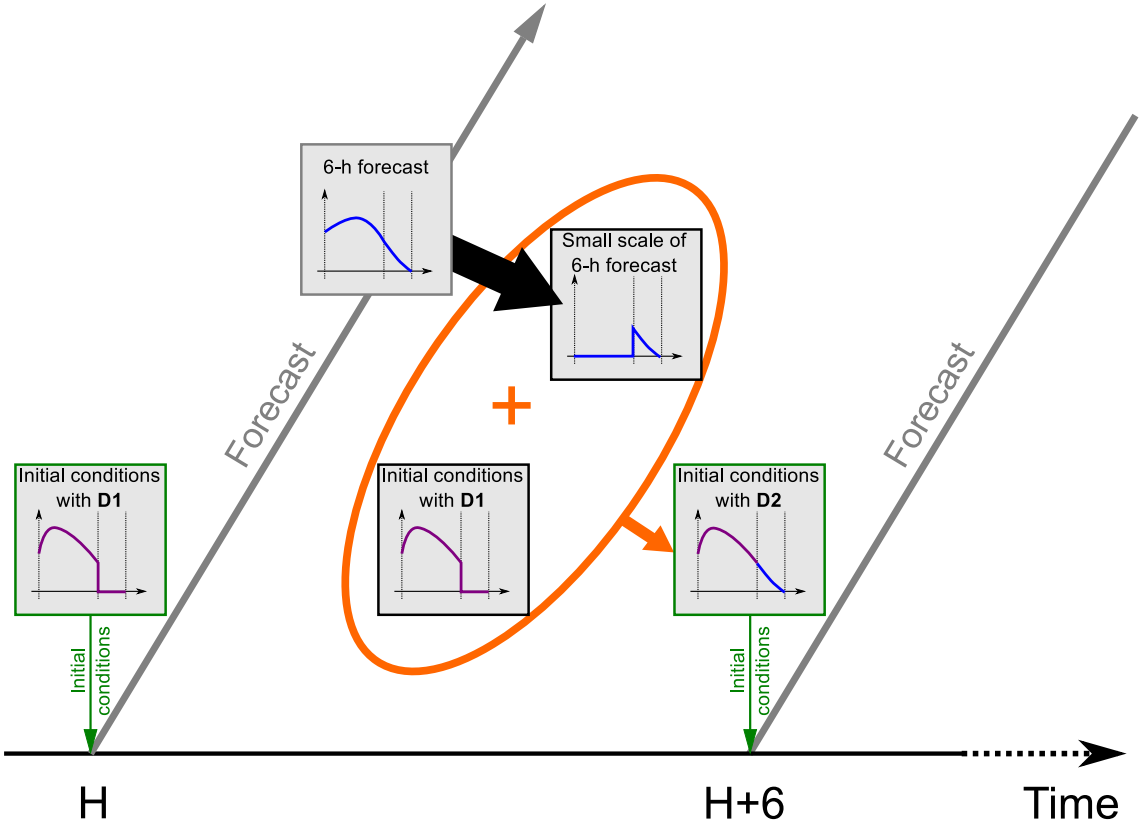

Figure 1. Schematic representation of D2 technique. Energy spectra are within small stamps.

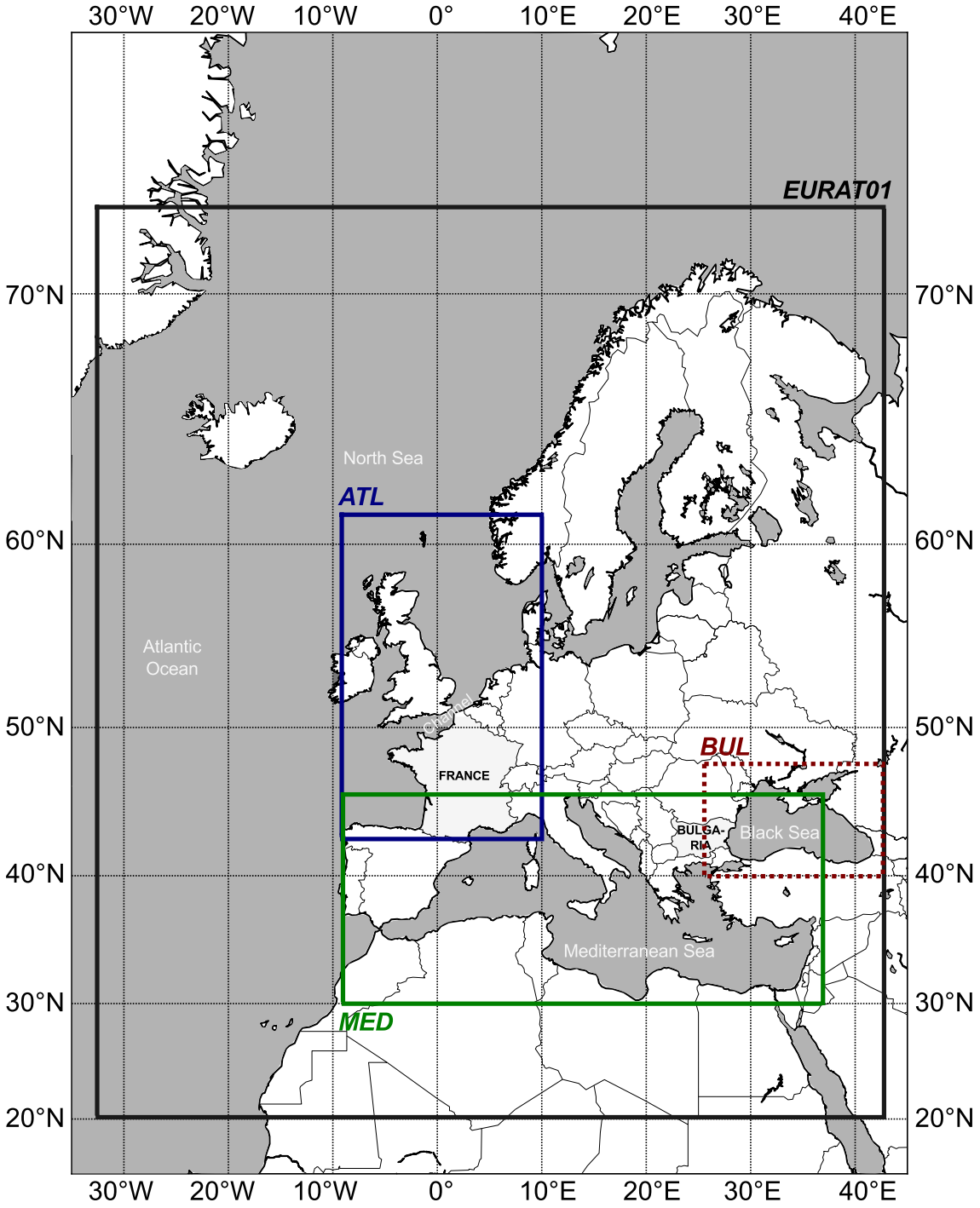

Figure 2. Locations of EURAT01 (black), ATL (blue), MED (green) and BUL (red) domains used in the study, respectively for European 0.1° resolution grid and Atlantic, Mediterranean and Bulgarian domains.

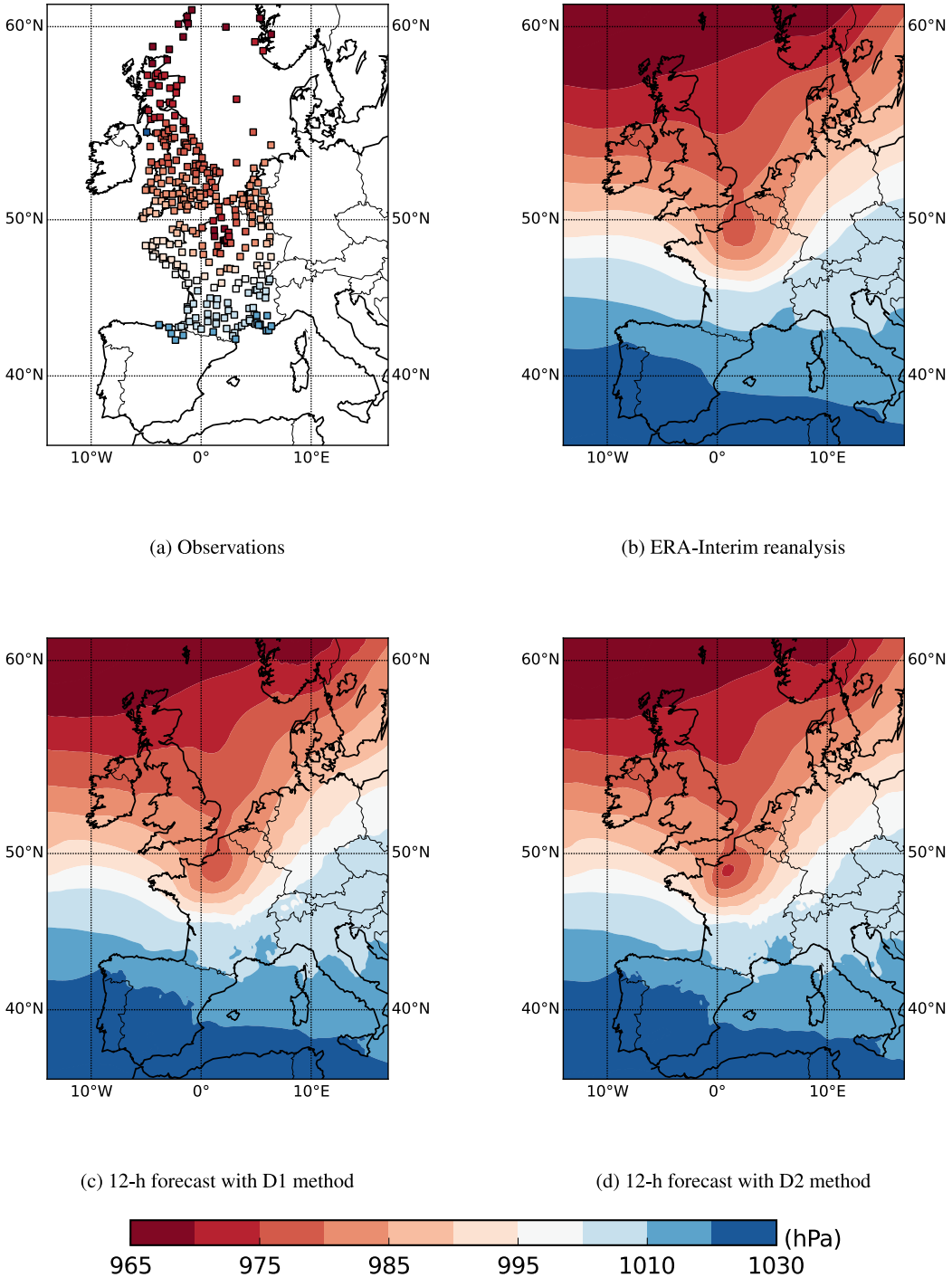

(a) Observations

(b) ERA-Interim reanalysis

(c) 12-h forecast with D1 method

(d) 12-h forecast with D2 method

Figure 3. Mean-sea level pressure (hPa) from observations (a) and ERA-Interim reanalysis at 06 UTC 26 December 1999 (b), from 12-h forecast using the D1 (c) and D2 (d) downscaling methods at 18 UTC 25 December 1999.

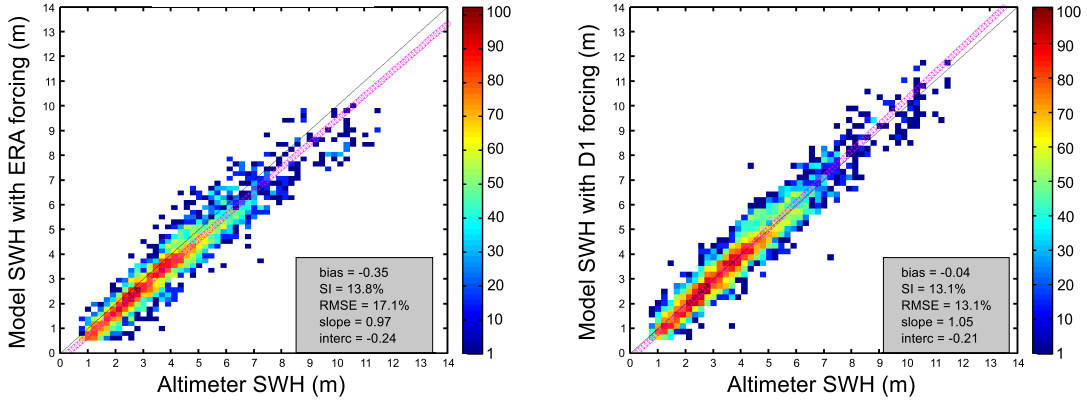

(a) with ERA-Interim forcing

(b) with D1 forcing

Figure 4. Scatter plots of significant wave heights of model MFWAM and altimeters (ENVISAT et Jason-1) for the 2004, 2007, 2008 and 2010 French storms. (a) and (b) stand for runs with interpolated ERA and D1 wind forcing, respectively.

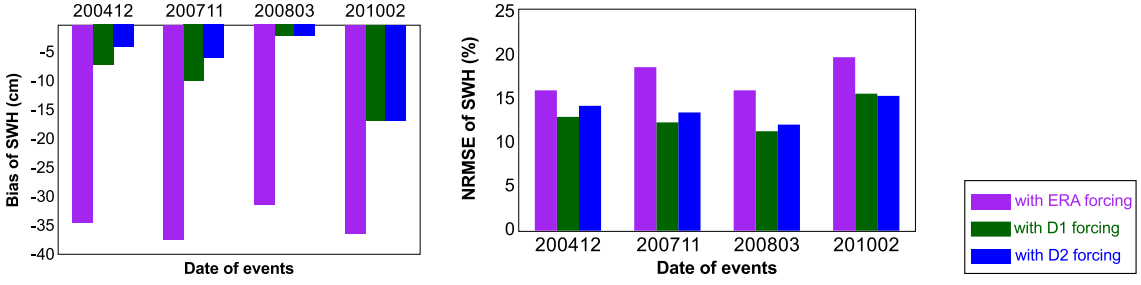

(a) Bias

(b) NRMSE

Figure 5. Variation of the bias (a) and the normalized root mean square error (NRMSE; b) of significant wave heights from the model MFWAM in comparison with the altimeters (ENVISAT et Jason-1) for the 2004, 2007, 2008 and 2010 French storms. Purple, green and blue colors stand for ERA, D1 and D2 forcing, respectively.

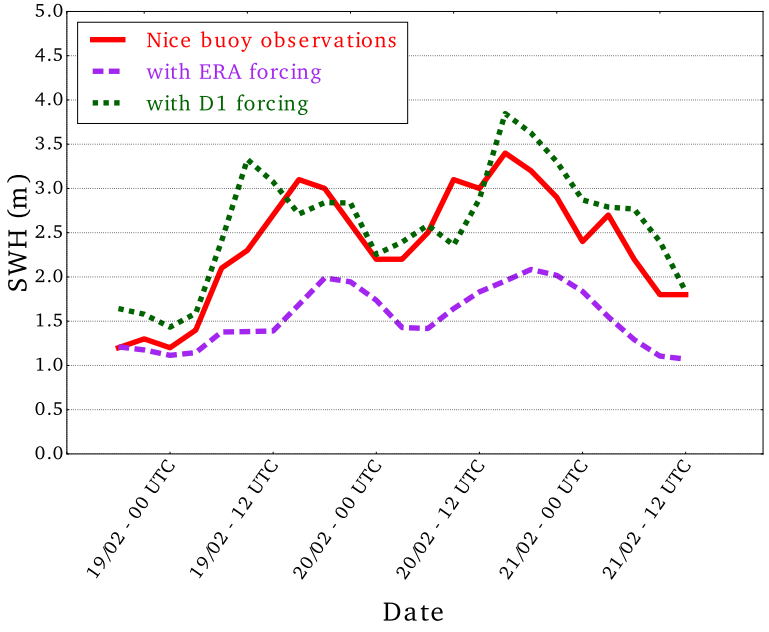

Figure 6. Time series of significant wave heights for the storm on February 2010 at Nice location (43.4° N and 7.8° E) in the Mediterranean sea. Purple and green colors stand for ERA and D1 forcing, respectively. Red line stands for Nice buoy observations.

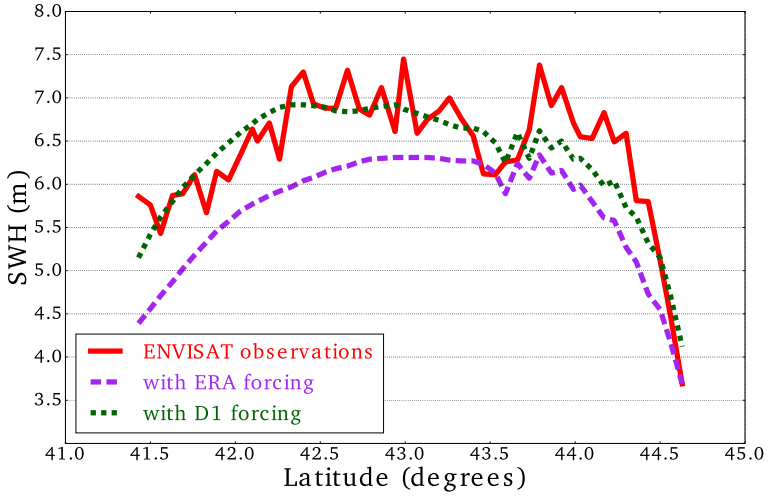

Figure 7. Comparison of the simulated significant wave heights with downscaled wind input and ERA wind input with the data from the ENVISAT track crossing the Western Black Sea at 20 UTC 7 February 2012. Purple and green colors stand for ERA and D1 forcing, respectively. Red line stands for ENVISAT observations.

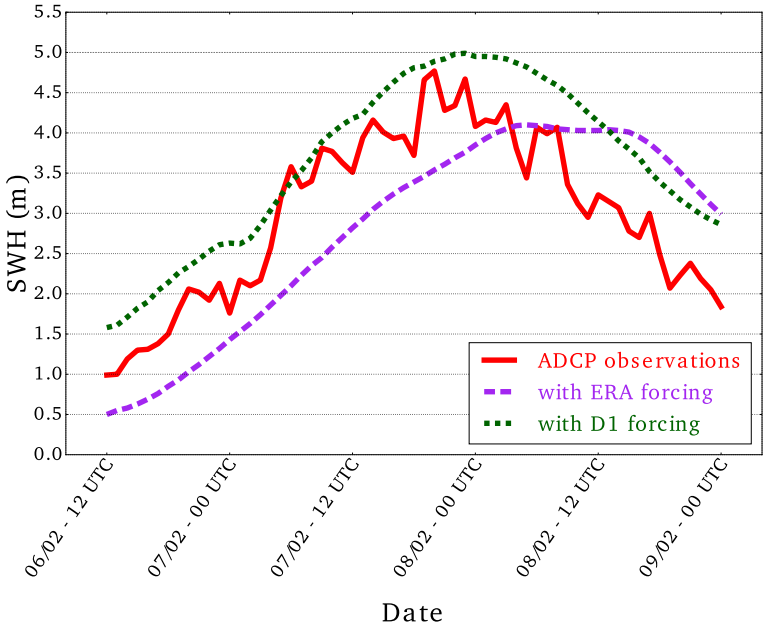

Figure 8. Comparison of the simulated significant wave heights using the two wind inputs (downscaled wind input D1 and ERA-Interim) with the data by ADCP located in the Western Black Sea coast at 20 m depth, during the storm of 7-8 February 2012. ADCP location coordinates: 43°04'49.13" N - 28°01'39.63" E. Purple and green colors stand for ERA and D1 forcing, respectively. Red line stands for ACDP observations.

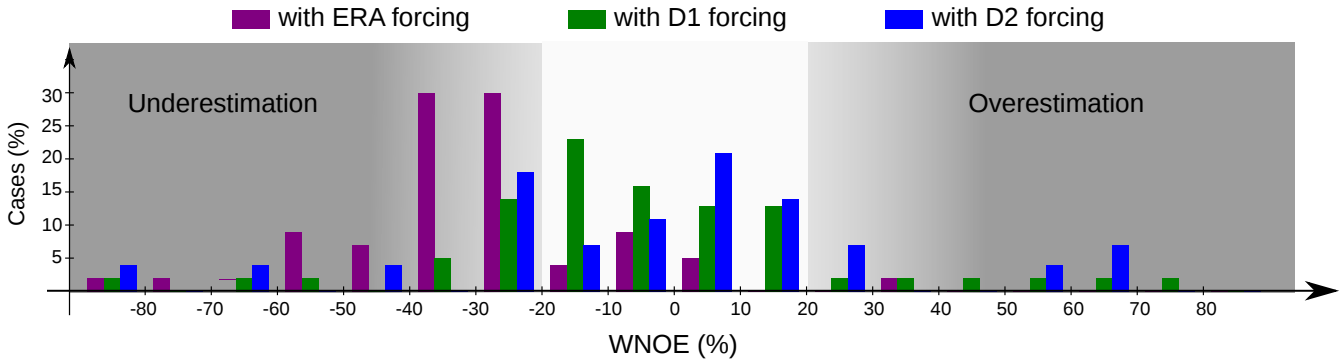

Figure 9. Percentage of cases depending of their $WNOE$ range when using ERA (purple), D1 (green) or D2 (blue) forcing. All the available observations with a maximum storm surge measurement are taken into account.

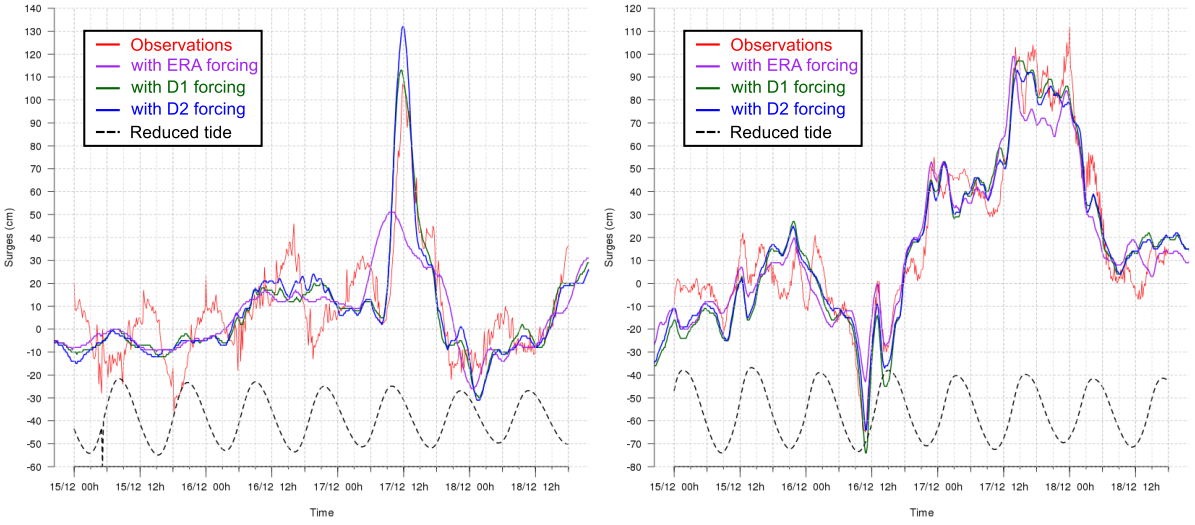

(a) St Malo

(b) Dunkerque

Figure 10. Storm surges (cm) at St Malo (a) and Dunkirk (b) from 14 December 2004 at 15 UTC to 19 December 2004 at 06 UTC. The measured surge (red line), the reconstructed surge by using the ERA forcing (purple line), the D1 forcing (green line) and the D2 forcing (blue line) are superimposed. The little oscillatory dotted line in the lower part of the graph is used to indicate the time of high and low tides.

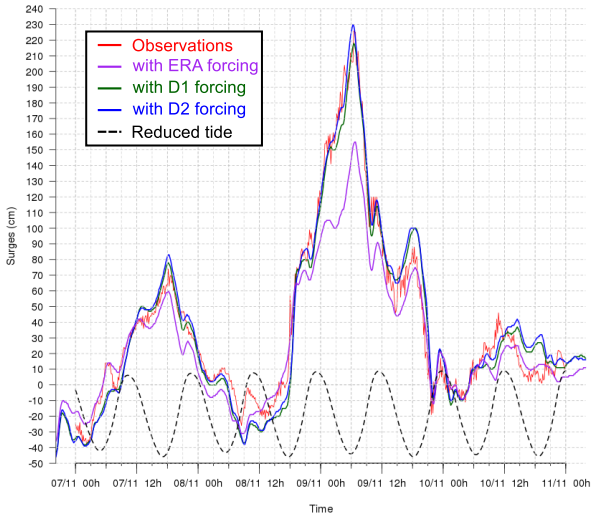

Figure 11. Storm surges (cm) at Dunkirk from 7 November 2007 at 15 UTC to 11 November 2007 at 06 UTC. The measured surge (red), the reconstructed surge by using the ERA forcing (purple), the D1 forcing (green) and the D2 forcing (blue) are superimposed. The little oscillatory dotted line in the lower part of the graph is used to indicate the time of high and low tides.

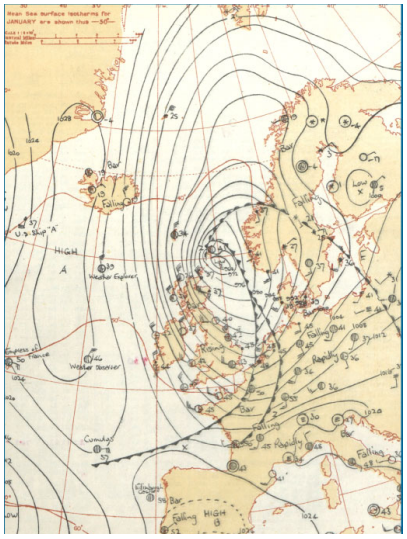

Figure 12. Surface pressure chart (hPa) at 06 UTC 1 February 1953. From hhttp://www.metoffice.gov.uk

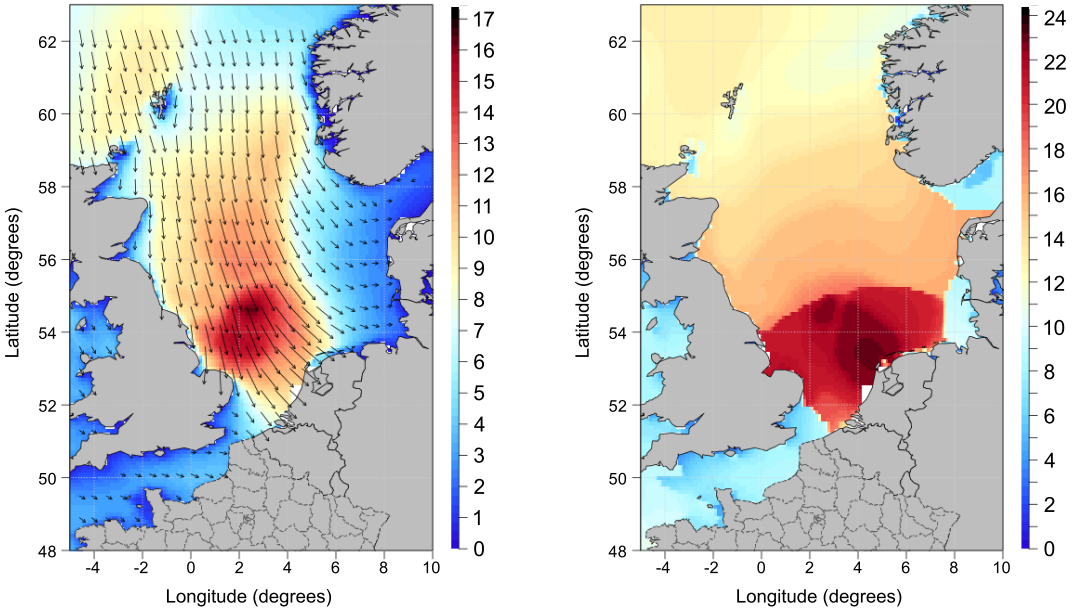

(a) Significant wave heights with D1 forcing

(b) Peak wave period with D1 forcing

Figure 13. Significant wave heights (m; a) and peak wave period (s; b) from the wave model MFWAM with D1 winds outputs on the peak of the storm at 00 UTC 1 February 1953. Mean Wave Direction is shown with black arrows in (a) when significant wave height are greater than 1.5 m.

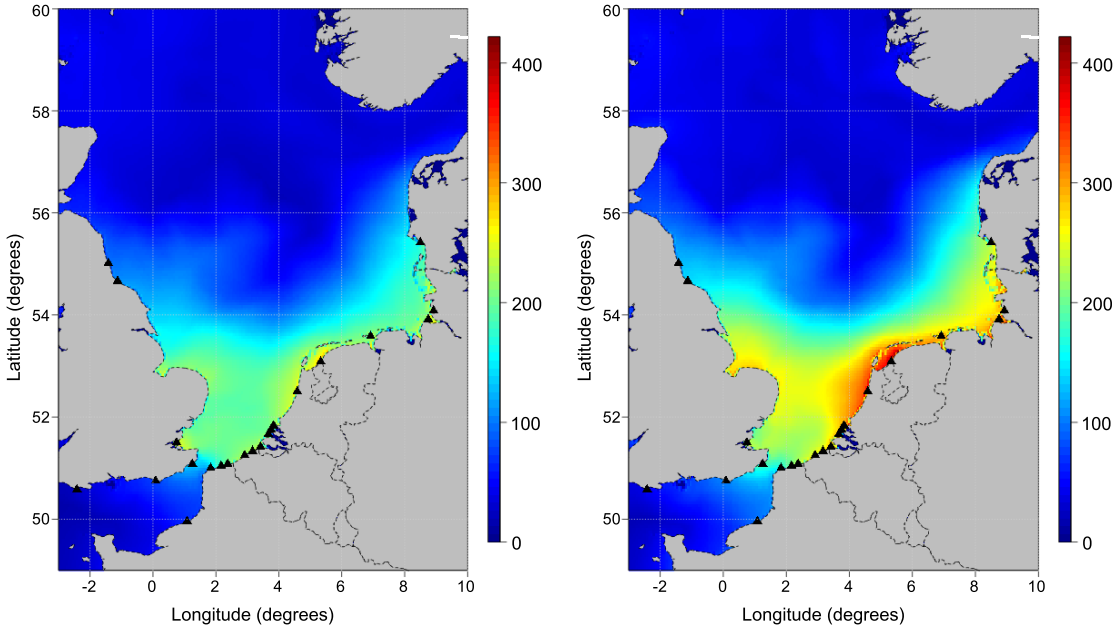

(a) with ERA-20C forcing

(b) with D1 forcing

Figure 14. Highest simulated storm surges (cm) obtained for the period from 30 January to 2 February 1953, with the ERA-20C forcing (a) and with the D1 forcing (b) along the southern part of the North Sea coast.

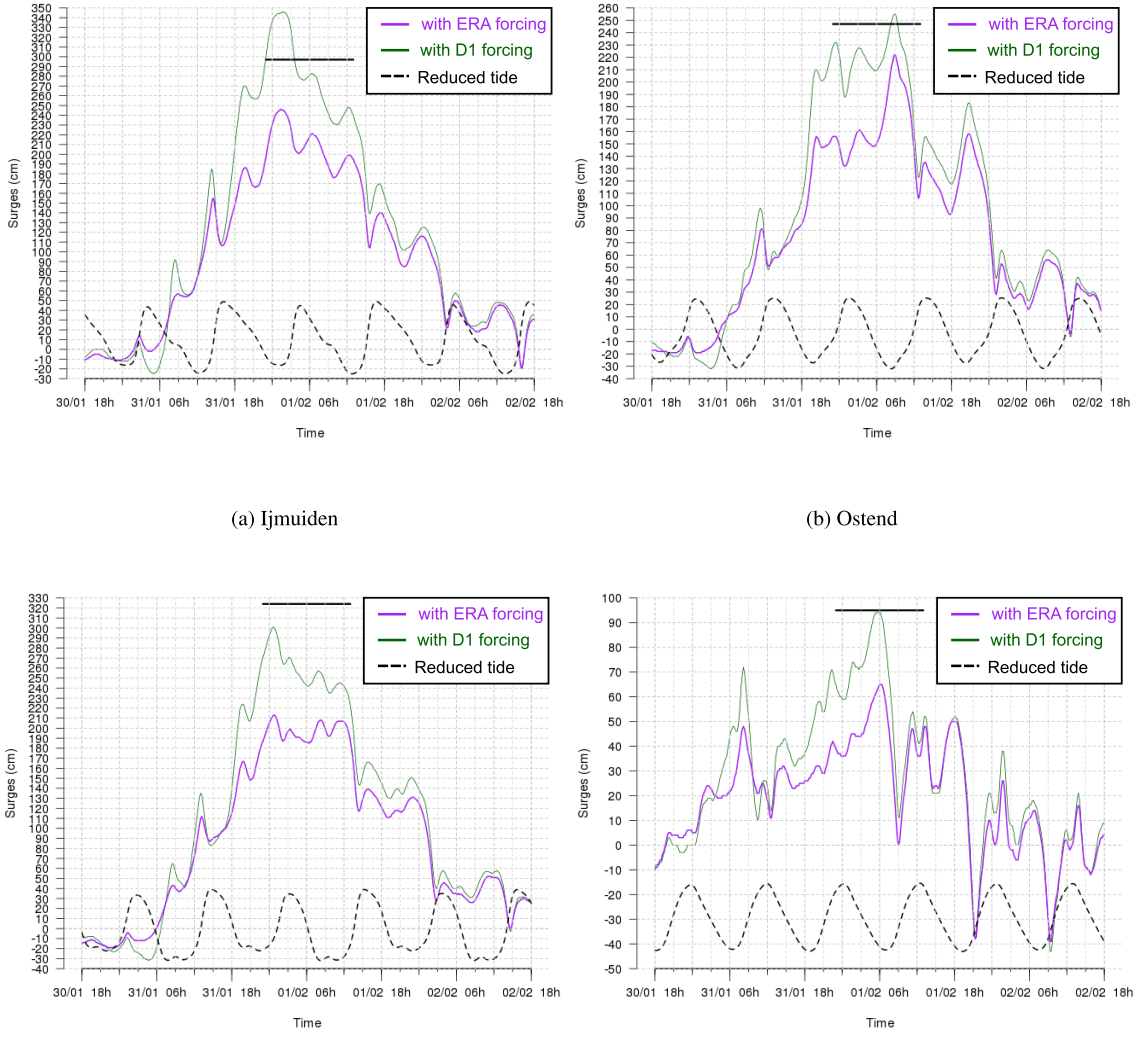

(a) Ijmuiden

(b) Ostend

(c) Brouwershavn

(d) Dieppe

Figure 15. Storm surges (cm) at Ijmuiden (Netherlands; a), Ostend (Belgium; b), Brouwershavn (Netherlands; c) and Dieppe (France; d) from 18 UTC 30 January to 18 UTC 2 February 1953. Two surges are represented: resulting of forcing with ERA-20C (purple) and with the D1 outputs (green). The maximum observed storm surge is added (horizontal plain black line). The tide level is indicated by the dashed black line (at a reduced scale).